Molecular Cancer Therapeutics

ATM Expression Predicts Veliparib and Irinotecan Sensitivity in Gastric Cancer by Mediating P53-Independent Regulation of Cell Cycle and Apoptosis

Vinod Vijay Subhash[1], Shi Hui Tan[2], Mei Shi Yeo[2], Fui Leng Yan[2], Praveen C. Peethala[1], Natalia Liem[2], Vaidehi Krishnan[1], and Wei Peng Yong[1,2]

Abstract

Identification of synthetically lethal cellular targets and synergistic drug combinations is important in cancer chemotherapy as they help to overcome treatment resistance and increase efficacy. The Ataxia Telangiectasia Mutated (ATM) kinase is a nuclear protein that plays a major role in the initiation of DNA repair signaling and cell-cycle check points during DNA damage. Although ATM was shown to be associated with poor prognosis in gastric cancer, its implications as a predictive biomarker for cancer chemotherapy remain unexplored. The present study evaluated ATM-induced synthetic lethality and its role in sensitization of gastric cancer cells to PARP and TOP1 inhibitors, veliparib (ABT-888) and irinotecan (CPT-11), respectively. ATM expression was detected in a panel of gastric cell lines, and the IC_{50} against each inhibitors was determined. The combinatorial effect of ABT-888 and CPT-11 in gastric cancer cells was also determined both *in vitro* and *in vivo*. ATM deficiency was found to be associated with enhanced sensitivity to ABT-888 and CPT-11 monotherapy, hence suggesting a mechanism of synthetic lethality. Cells with high ATM expression showed reduced sensitivity to monotherapy; however, they showed a higher therapeutic effect with ABT-888 and CPT-11 combinatorial therapy. Furthermore, ATM expression was shown to play a major role in cellular homeostasis by regulating cell-cycle progression and apoptosis in a P53-independent manner. The present study highlights the clinical utility of ATM expression as a predictive marker for sensitivity of gastric cancer cells to PARP and TOP1 inhibition and provides a deeper mechanistic insight into ATM-dependent regulation of cellular processes. *Mol Cancer Ther; 15(12); 3087–96. ©2016 AACR.*

Introduction

The cellular response to DNA damage is an important event that involves transcriptional alteration and activation of checkpoint pathways thereby causing a delay in cell cycle progression. This delay provides sufficient time for the cell to assess and repair the damage before re-entering the cell cycle (1). The Ataxia Telangiectasia Mutated (ATM) kinase is a nuclear protein that plays a major role in the initiation of DNA repair signaling and cell-cycle check points during DNA double-strand breaks (DSB; ref. 2). ATM not only mediates cellular responses to DNA repair, but also regulates cellular senescence induced by persistent DNA damage (3). Germline and somatic alterations in ATM have been revealed as a predisposing factor for cancer development (4). In recent years, ATM expression has also been shown to be associated with poor survival and drug resistance in cancer patients (5, 6). As cancer cells often have specific abnormalities in the DNA damage response, therapeutic strategies based on utilizing such properties have been developed (7, 8). Chemotherapeutic agents and radiotherapy exert their cytotoxic effects on cancer cells by inducing DNA DSBs (9, 10). Several inhibitors that block specific DNA damage responses or repair proteins have been tried not only as sensitizing agents in combination with DNA-damaging agents but also as single agents against cancers with defects in specific DNA repair pathways. A deficiency of ATM function has been reported in many tumor types including colon cancer, breast cancer, lung cancer, and gastric cancer (11–14). *In vitro*, cell lines with high ATM expression showed higher resistance to DNA-damaging agents (15), whereas reduced ATM expression was found to be associated with higher sensitivity (16). Therefore, ATM deficiency could act as a selective characteristic in tumor for therapies targeting DNA repair pathways.

The ability of cells to trigger check points and DNA repair pathways has a major influence in the clinical efficacy of anticancer agents. Veliparib (ABT-888) is a PARP 1 and 2 inhibitor, and its chemical structure is previously defined (17). Veliparib targets PARP-mediated multiple DNA damage response pathways and was shown to have promising effects in the treatment

[1]Cancer Science Institute of Singapore, Yong loo Lin School of Medicine, National University of Singapore, Singapore. [2]Department of Haematology-Oncology, National University Hospital, Singapore.

Note: Supplementary data for this article are available at Molecular Cancer Therapeutics Online (http://mct.aacrjournals.org/).

Natalia Liem was not available to confirm co-authorship, but the corresponding author Wei Peng Yong affirms that Natalia Liem contributed to the paper, and thus, confirms Natalia Liem's co-authorship status.

Corresponding Author: Wei Peng Yong, National University Hospital, 5 Lower Kent Ridge Road, Singapore 119074, Singapore. Phone: 65-67795555; Fax: 65-67775545; E-mail: wei_peng_yong@nuhs.edu.sg

doi: 10.1158/1535-7163.MCT-15-1002

of ovarian and breast cancers (18). PARP-1 plays an important role in the modulation of DNA damage repair and hence is a potential target to synergize DNA-damaging drugs. PARP-1 binds to the damaged region of DNA and enables repair proteins to fill in the missing nucleotides, thereby facilitating DNA repair. Inhibition of PARP1 could lead to an increase in single-strand breaks (SSB), and if left unrepaired, these SSBs would lead to the formation of increased DSBs and in turn increased cell death (19, 20). However, cells contain alternative mechanism for DNA damage repair in the absence of PARP activity. In this regard, loss of function or mutations in proteins involved in such alternative DNA repair mechanisms would further enhance the efficacy of PARP inhibitors. This brings about the concept of "synthetic lethality" where inactivation of complementary DNA repair pathways has been proposed as a promising therapeutic option (21). Recently, ATM deletion was shown to confer sensitivity to PARP inhibition in breast cancer cells (22). Also, Kubota and colleagues (23) demonstrated ATM deficiency as a potential predictive biomarker for PARP-1 inhibitor activity in gastric cancer harboring disruption of p53. Studies have also shown other strategies by combining PARP-1 inhibitors with the DNA-damaging topoisomerase I inhibitor, Irinotecan (CPT-11; ref. 24). Topoisomerases are widely used targets for the development of anticancer drugs in solid tumors (25). CPT-11 binds to the Top I-DNA complex and prevents re-ligation of double-stranded DNA during DNA replication. This results in Top1 being trapped on a nicked DNA intermediate in replicating cells and thereby causing cell death (26). The synergy between PARP- and Top1-inhibitors was recently confirmed by clinical data (27–29). It is likely that disruption of DNA repair by PARP inhibitor sensitizes the cells to the DNA damage effects of TOP1, thereby causing an enhancement in overall cell death (30). However, a deeper insight into the underlying mechanisms for these findings has been limited to that provided by a few biochemical studies (27, 31).

Identification of the individualities in DNA repair pathways that reflects changes in DNA repair activities in tumor cells is advantageous in developing effective therapeutic strategies (32). Because synergism of PARP and TOP1 inhibitors can potentially enhance therapeutic benefits, the current study is aimed at elucidating the combinatorial effects of ABT-888 and CPT-11 in gastric cancer. Here, we investigate the correlation between ATM-induced synthetic lethality and sensitivity of gastric cancer cells to ABT-888 and CPT-11 and also provide a mechanistic insight into the ATM-dependent regulation of cell-cycle progression and apoptosis.

Materials and Methods

Cell lines and drug treatment

Gastric cancer cell lines IM95, IST1, NUGC4, TMK1, and YCC3 were purchased from Health Science Research Resources Bank. MKN45 and MKN1 were obtained from DUKE NUS. SNU16 was purchased from the American Type Culture Collection (ATCC). HGC27 was purchased from National Collection of Type Cultures (NCTC). AZ521 was obtained from Japanese Collection of Research Bio-resources Cell Bank (JCRB). The cell lines were authenticated by the respective cells banks by short random repeat profiling. All the cell lines were cultured in RPMI 1640 supplemented with 10% (v/v) FBS, 1% (v/v) penicillin and streptomycin (Gibco) at 37°C in 5% CO_2 incubator. ABT-888 and CPT-11 were obtained from Selleckchem and Hospira, respectively, and used for *in-vitro* and *in-vivo* efficacy studies.

Cell proliferation assay

A total of 2,000 cells were seeded on each well of flat bottom 96-well plates (nunclon) and incubated for 24 hours. For chemosensitivity analysis, a dilution series containing the appropriate drug concentrations was applied at final drug concentrations of 0.1; 1; 10; 100; and 1,000 μmol/L and incubated for 72 hours in a humidified incubator under an atmosphere of 5% CO_2 at 37°C. Cell proliferation was estimated using the CellTiter 96 Aqueous Non-Radioactive Cell Proliferation Assay (Promega) according to the manufacturer's instructions. The absorbance of samples at 590 nm (A590) was measured with a Tecan Infinite plate micro plate reader, and results were expressed as the mean of triplicates in percentage. All experiments were performed independently and repeated 3 times.

Combination index

Combination index (CI) was calculated using Calcusyn software 2.0. The reaction was classified as synergistic when CI < 1 and antagonistic when CI > 1. The mean of affected fraction for triplicate was used for analysis. Experiments were performed independently at least 2 times

Immunohistochemistry staining and scoring

Cells were cytospun onto glass slides and fixed with 4% formaldehyde for 10 minutes. Fixed cells were incubated with H_2O_2 (Sigma-Aldrich) for 10 minutes, blocked with 1% BSA (Sigma-Aldrich) for 1 hour, and permeabilised with 0.2% triton X100 (Thermo Scientific) for 10 minutes. The slides were then incubated with 1:200 primary rabbit monoclonal antibody (Abcam) at 4°C overnight. Following which, slides were incubated with anti-rabbit antibody for 1 hour and then stained with 1:50 chromogen substrate (Dako) for 3 minutes.The counterstaining was done with hematoxylin (Dako) for 1 minute followed by ammonium hydroxide (Sigma-Aldrich) for 3 minutes. The slides was immersed serialy in 70% EtOH, 95% EtOH, and 100% EtOH for 5 minutes and then immersed in Histoclear (National Diagnosics) before proceeding to microscopic analysis for ATM expression. Brown color in nucleus was classified as positive staining for ATM. Five random fields were counted for each cell lines to calculate the percentage of ATM-positive population. Cells were classified into high or low ATM expression according to their ATM percentage, with the median serving as a cutoff point. Cells with >25% positive cell population were classified under high ATM level, whereas cells with $\leq$25% were classified under low ATM expression

Small interfering RNA transfection

Human ATM and p53 siRNA plasmids were purchased from Santa Cruz Biotechnology. HGC27 cells (1×10^5 cells/well) were plated in 6-well plates and grown in 2 mL RPMI-1640 medium with 10% FBS. Transfections of siRNA and control vectors were performed with jetPrime (Invitrogen) according to the manufacturer's instructions. Cell lysates were collected at 36 hours after transfection followed by detection of ATM and P53 expression by Western blot analysis.

MTT cell viability assay

HGC 27 cells were seeded on to 96-well plates at a density of 2×10^3 cells/well. The cells were treated with IC_{50} concentrations of CPT-11 and ABT-888, either as single agent or in combination. After incubation for 24 hours at 37°C, 20 μL of MTT (2 mg mL^{-1}; Sigma) was added and incubated again for 4 hours. The formazan MTT precipitate was then dissolved in 200 μL of dimethylsulphoxide, and the absorbance was measured at a wavelength of 490 nm.

Immunofluorescence assay

Cells were seeded at a density of 2×10^4 cells/well onto coverslips in a 24-well plate. Following 30 minutes of fixation in 4% paraformaldehyde, 10 minutes of permeabilization with 0.5% Triton X-100 solution, and 1 hour of blockage with 5% BSA in PBS, cells were incubated with primary monoclonal mouse anti-human γH2AX antibody (Cell Signaling Technology) for 2 hours, and Alexa Fluor 488 polyclonal goat anti-rabbit IgG (H+L) secondary antibody (green; Invitrogen Life Technologies) for 1 hour. DAPI was used to stain the nuclei. All images were captured using a confocal laser microscope (Leica TCS SP5; Leica).

Cell-cycle assay

Cells were seeded at a density of 2×10^5 cells in 6-well plates. After overnight incubation, the cells were treated for 24 hours with respective drugs, harvested, and fixed in 70% ethanol. Following fixation, cells were treated with RNase (5 μg mL^{-1}; Ambion) and stained with propidium iodide (50 μg mL^{-1}; Life Technologies) for 30 minutes at 37°C. For each sample, a total of 10,000 events were analyzed for DNA content by flow cytometry on a BD LSR II (BD biosciences). The cells in G_1, S, and G_2–M phases were quantified using FlowJo software (version vX 0.7).

Western blot analysis

Cells were washed with ice-cold PBS, and whole-cell lysates were prepared using CelLytic buffer (Sigma-Aldrich). Protein (20 μg) was electrophoretically separated on 12% SDS-PAGE. Western blots were performed with the primary antibodies: anti-ATM (Santa Cruz Biotechnology), anti-p53, anti-phosphoChk2, anti-p21 Waf1/Cip1 (12D1), anti-PUMA, anti-GAPDH (Cell Signaling Technology) and the corresponding secondary antibodies: anti-rabbit/mouse IgG and HRP-Linked (Cell Signaling Technology). The signals were visualized by ECL reagent (Amersham ECL Plus Western Blotting Detection System; GE Healthcare), followed by exposure to chemiluminescence film (Amersham Hyperfilm ECL; GE Healthcare). The Western blot analyses were repeated twice for each protein tested.

Lentiviral-mediated stable knockdown of ATM in HGC27 cells

Lentiviral constructs with three different human ATM shRNA's and scramble control shRNA were purchased from Origene Technologies. Lentiviruses were prepared by transient cotransfection with lentiviral plasmids into 293T cells using Lipofectamine 2000 as previously described (33). For generating stable ATM knockdown (kd) cells, 2 days after transfection, supernatants containing viral particles were harvested and used to infect HGC27 cells in RPMI supplemented with 8 μg/mL of polybrene as per the manufacture's protocol. Seventy-two hours after infection, the medium was changed to the selection RPMI with 10% FBS and supplemented with puromycin 0.1 mg/mL to screen stable cell lines for further assay. Three weeks later, the cell clones were screened for ATM kd using RT-PCR. The primers used for ATM amplification are described in Supplementary Table S1.

Xenograft model of gastric cancer

Six-week-old NOD-SCID mice ($n = 50$) were injected subcutaneously with HGC27 control or HGC27 ATM stable kd cells (5×10^6 cells) suspended in Matrigel (BD biosciences). Five animals were randomly assigned to each treatment group. (1) Vehicle (0.9% NaCl and 0.5 % DMSO, Ph-4), (2) Irinotecan; 20 mpk, *i.p*, 2x week, (3) Veliparib; 50 mpk, oral-gavage, 2x week, (4) combination of irinotecan and veliparib. Treatment was continued for 2 weeks, and tumor growth was followed by bi-weekly measurements of tumor diameters with a vernier caliper, and tumor volume (TV) was calculated according to the formula: $TV = (W^2 \times L)/2$ mm^3, where "W" is the width and "L" is the length. The antitumor activity was assessed as rumor growth inhibition percentage (TGI%) in treated versus control mice, calculated as follows: TGI% = 100 – (mean TV treated/mean TV control × 100). The experiments were performed in accordance with Institutional Animal Care and Use Committee guidelines. Mice were sacrificed if they had a tumor greater than 1.5 cm in diameter, if total tumor burden was greater than 10% of body weight, or if a tumor ulcerated or interfered with mobility.

Statistical analysis

Reads per kilobase of transcripts per million (RPKM) expression and clinical information of 265 gastric adenocarcinoma primary tumor tissue samples from The Cancer Genome Atlas (TCGA) database (https://tcga-data.nci.nih.gov/docs/publications/stad_2014/) were analyzed. Pearson correlation analysis was performed to assess association between any two genes of interest. The analyses were computed using R statistical packages (www.r-project.org). All statistical analyses were considered significant when P values <0.05.

Results

High ATM expression is associated with increased drug resistance

Figure 1A shows IHC staining of nuclei-bound ATM in gastric cancer cells. Varied expression level of ATM was found across cell lines among which IM95 showed the least detectable expression. Among the 10 cell lines tested, 5 demonstrated low ATM expression (IM95, AZ521, NUGC4, SNU16, and MKN45), whereas the remaining 5 cell lines (TMK1, YCC3, MKN1, HGC27, and IST1) showed high ATM expression. To determine the efficacy of ABT-888 and CPT-11 in these gastric cancer cell lines, IC_{50} drug responses were analyzed (Table 1). In general, the cell lines appeared to be relatively more sensitive to TOP1 inhibitor as compared with PARP inhibitor, with IC_{50} ranging between 1–30 μmol/L and 24–122 μmol/L for CPT-11 and ABT-888, respectively. Interestingly, ATM expression was found to be associated with reduced drug sensitivity as cell lines with high ATM expression exhibited significantly high IC_{50} values to both drugs (ABT-888 $P \leq 0.05$, CPT-11 $P \leq 0.01$; Fig. 1B). The linear regression model showed a positive correlation between ATM expression level and CPT-11 chemosensitivity ($R^2 = 0.8643$). ABT-888 also showed a positive correlation between chemosensitivity and ATM expression; however, the association was found to be relatively weak ($R^2 = 0.3035$; Fig. 1C).

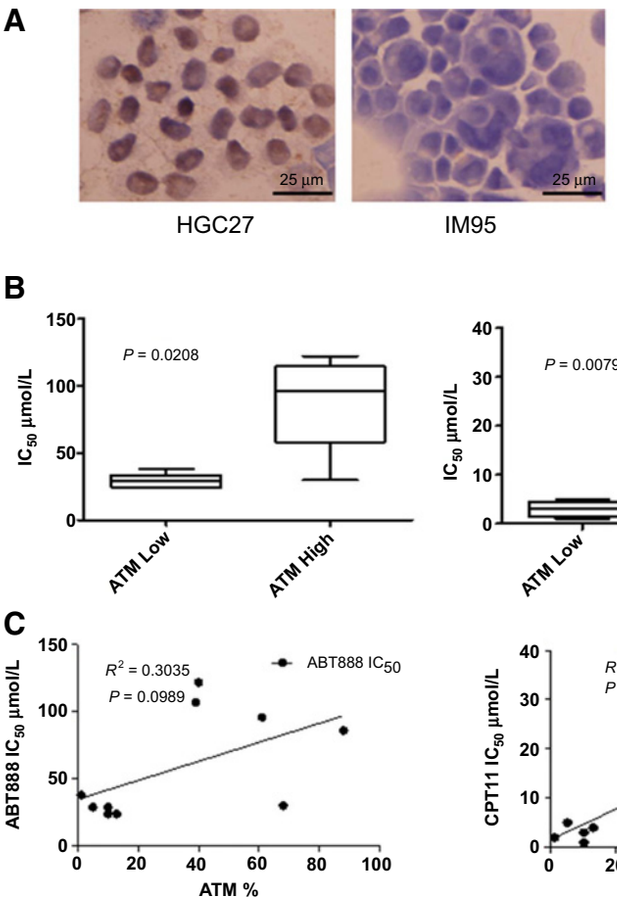

Figure 1.
A, IHC staining of ATM expression: Positive ATM staining, indicated by brown color staining in nucleus, can be observed in HGC27. Negative staining, indicated by blue color staining in the nucleus, can be observed in IM95. **B,** ATM expression and drug sensitivity: ABT-888 and CPT-11 IC_{50} for 10 gastric cell lines were determined and plotted against their ATM expression levels. **C,** Linear regression of IC_{50} of CPT-11 vs. ATM percentage.

Combination drug treatment results in synergistic interaction between ABT-888 and CPT-11

To further determine whether ATM influences the synergistic interaction between ABT-888 and CPT-11, two cell lines were selected based on their ATM expression levels (IM95 showing low ATM expression; HGC27 showing high ATM expression). Interestingly, combinatorial treatment using ABT-888 and CPT-11 resulted in a synergistic interaction across both cell lines (CI < 1). However, cell line with higher ATM expression (HGC27) showed a higher synergistic response to the drug combination at ED50, 75, and 90 as compared with cell line that exhibited lower ATM expression (IM95; Table 2A). Of interest, combinatorial drug treatment was also found to lower drug IC_{50} when compared with single-agent treatments of ABT-888 and CPT-11 (Table 2B). HGC27 showed a higher synergistic response to combination drug therapy with both ABT-888 and CPT-11 showing a significant decrease of 50.9% each in IC_{50} while comparing with single-agent treatments. In contrast, IM95 showed a lower synergistic response following combinatorial drug therapy, with ABT-888 and CPT-11 showing a 36.4% and 25.3% reduction in IC_{50} respectively.

CPT-11 and ABT-888 synergistically enhance H2AX phosphorylation and apoptosis

To understand the synergistic effect of PARP and TOP-1 inhibitors in cells with high ATM expression, HGC27 cells were treated with ABT-888 and CPT-11 either as single agent or in combination. Figure 2A shows the accumulation of γH2AX loci

Table 1. IC_{50} of ABT888 and CPT11 and on 10 gastric cancer cells and their percentage ATM protein

	Cell lines	ABT-888 (μmol/L)	CPT-11 (μmol/L)	ATM%
1	IM95	38	2	1
2	NUGC4	29	5	5
3	SNU16	24	3	10
4	AZ521	29	1	10
5	MKN45	24	4	12.9
6	TMK1	107	17	39
7	YCC3	122	22	40
8	MKN1	96	18	61
9	HGC27	30	18	68
10	Ist1	86	30	88

Table 2. (A) Summary of CI and (B) percentage decrease in IC_{50} of gastric cell lines to ABT-888 and CPT-11, after combinational drug treatment

A

Cell lines		CI		
	ATM expression	ED50	ED75	ED90
IM95	Low	0.8	0.8	0.8
HGC27	High	0.6	0.3	0.2

B

Cell line	%Decrease of ABT-888 IC_{50}	%Decrease of CPT-11 IC_{50}
IM95	36.4	25.3
HGC27	50.9	50.9

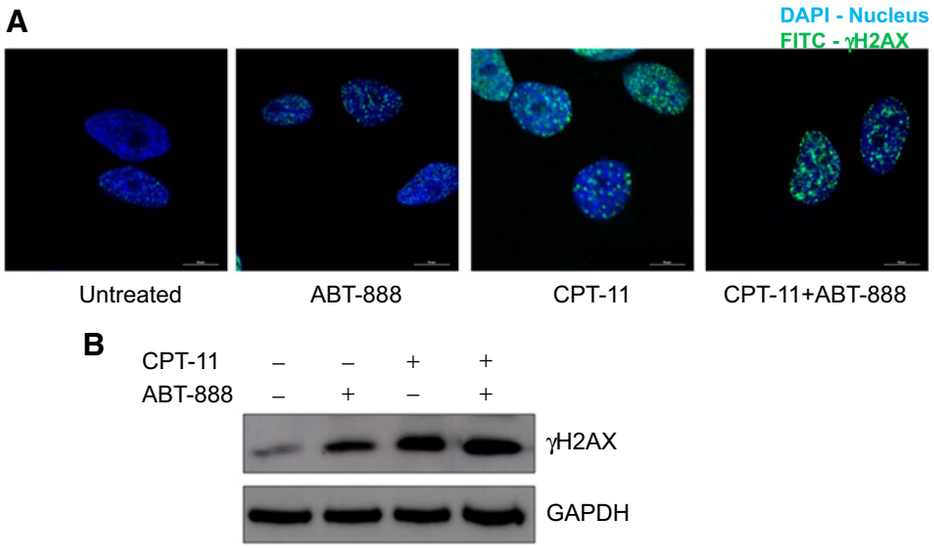

Figure 2.

A, Foci formation assay: Confocal microscopy images of γH2AX foci formation (green) in HGC27 cells treated with IC_{50} concentrations of ABT888 and CPT11 either as single agent or in combination for 24 hours. Untreated cells served as experimental controls. Slides were counterstained with DAPI to visualize nuclei (blue). **B,** HGC27 cells were left untreated or treated with IC_{50} concentrations of ABT888 and CPT11 either as single agent or in combination for 24 hours. DNA damage as indicated by phosphorylation of H2AX (Ser139) was assessed by immunoblotting. GAPDH represents loading controls.

in the nuclei of HGC27 cells. Treatment with CPT-11 resulted in an accumulation of γH2AX loci, hence suggesting enhanced DNA damage. Although PARP inhibition alone using ABT-888 did not cause any significant DNA damage, combinatorial treatment of CPT-11 and ABT-888 leads to a greater increase in DNA damage as shown by enhanced γH2AX loci formation. Figure 2B shows DNA damage–induced phosphorylation of H2AX in HGC27 cells. A significant upregulation of γH2AX was observed in CPT-11–treated cells as compared with the basal level observed in untreated and ABT-888–treated cells. Consistently, a further increase in γH2AX expression was observed in cells treated with the combination of ABT-888 and CPT-11. The effect of CPT-11– and ABT-888–induced DNA damage insult in cell-cycle progression was also investigated. Figure 3 indicates the cell-cycle profiles and the percentage of cells in each phase of the cell cycle, under different treatment conditions. Cells treated with ABT-888 and CPT-11 showed a pronounced increase in G_1 and G_2–M phases, whereas combinatorial drug treatment resulted in an increase of cell population in the G_1 phase concomitant with

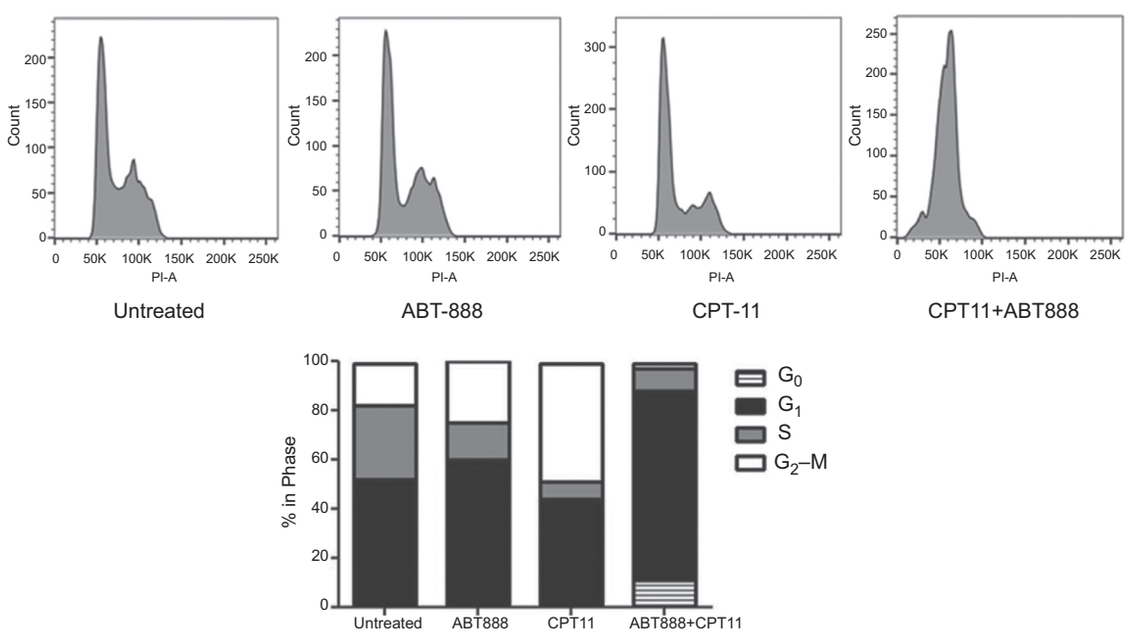

Figure 3.

Cell-cycle analysis of HGC-27 cells 24 hours after treatment with [IC_{50}] of ABT-888 or CPT-11 either as single agent or in combination. The percentage of cells in each phase of the cell cycle was calculated as the ratio of events in each phase to the total number of events. A total of 10,000 events were analyzed for each sample.

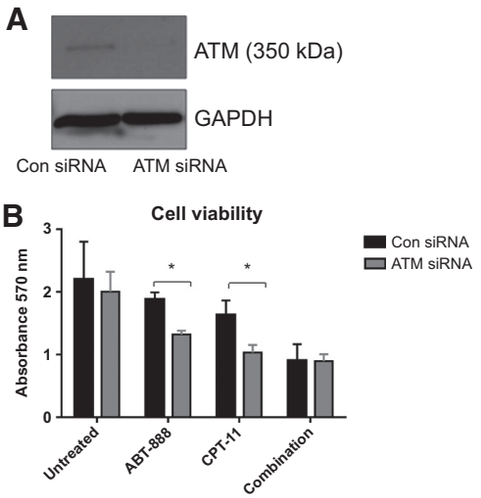

Figure 4.

A, ATM was knocked down in HGC27 cells using targeted siRNAs; Con siRNA: scrambled controls, ATM siRNA: knockdown variant; and its effect in protein expression was detected by immunoblot analysis. **B,** MTT assay: Viability of control and ATM knockeddown cells were evaluated under different treatment condition. Untreated cells served as experimental controls. Results are representative of two independent experiments, and error bars indicate SDs. *, $P < 0.05$ is considered significant.

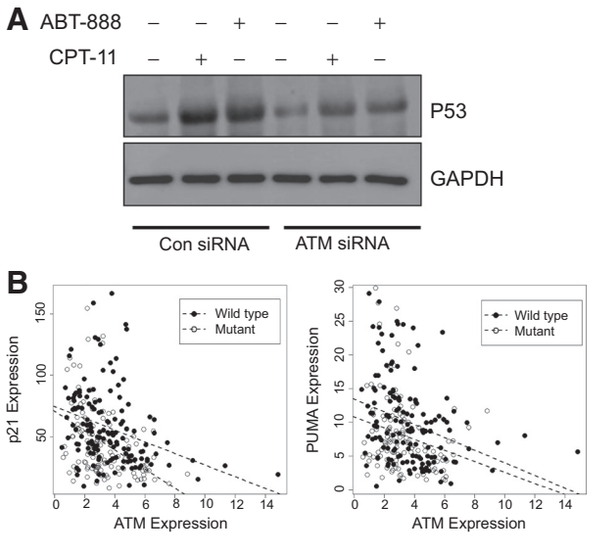

Figure 5.

A, Immunoblot analysis of p53 expression. HGC27 cells (Con siRNA, scrambled control; ATM siRNA, ATM kd variant) were treated with IC_{50} concentrations of ABT888 and CPT11 either as single agent or in combination for 24 hours. **B,** Scatterplots depict significant inverse relationships between ATM and P21, and ATM and PUMA in patients with wild-type (blue) mutant (red) p53 expression. Correlation between ATM and P21 expression—P53 wild-type: $r = -0.32$, P value = 0.0001; P53 mutants: $r = -0.39$, P value = 1.33e−05. Correlation between ATM and PUMA expression—p53 wild-type: $r = -0.31$, P value = 0.0002; P53 mutant: $r = -0.25$, P value = 0.006.

significantly higher proportion of apoptotic cells (G_0 phase). The data suggest enhanced sensitivity of HGC 27 cells to the combination of ABT-888 and CPT-11 as compared with single-agent treatment.

ATM knockdown enhanced ABT-888 and CPT-11 sensitivity in gastric cancer cells

ATM expression was knocked down in HGC27 cells using siRNAs. A downregulation of ATM mRNA (Supplementary Fig. S1) and protein expression (Fig. 4A) was observed in siRNA-treated cells as compared with cells treated with nontargeting control siRNAs. Treatment of HGC27 cells with ABT-888 and CPT-11 caused a decrease in overall cell viability. Interestingly, kd of ATM expression leads to a further decrease in cell viability, hence suggesting enhanced sensitivity to PARP and TOP1 inhibitors ($P < 0.05$; Fig. 4B). Of note, ABT-888 and CPT-11 in combination caused a synergistic effect that led to enhanced sensitivity in both ATM-expressing and nonexpressing cells.

ATM exhibits an inverse correlation with P21 and PUMA expression in gastric cancer

HGC27 cells treated with TOP1 and PARP inhibitors showed significant upregulation of P53 expression (Fig. 5A). However, kd of ATM expression leads to a decrease in P53 levels. Our data are consistent with previous studies (34, 35) that showed a contributory role of ATM in P53 expression. Although analysis of TCGA public datasets revealed no significant association between ATM and P53 expression in gastric cancer patients (data not shown), an inverse correlation was shown to exist between ATM and expression of P53 downstream targets p21 and PUMA (Fig. 5B). Interestingly, this association appeared to be independent of p53 as patients with both wild-type and mutated P53 expression showed a significant inverse correlation between ATM and P21 expression, and ATM and PUMA (Table 3).

ATM mediates P53-independent regulation of apoptotic and cell-cycle signaling in gastric cancer cells

To further determine the role of P53 in ATM-dependent regulation of cellular events, P53 expression was knocked down in HGC27 cells using siRNAs. Figure 6A shows a reduction in P53 expression in siRNA-targeted cells as compared with the nontargeted cells. The effect of ATM and P53 kd in check point arrest and apoptosis of gastric cancer cells was also investigated (Fig. 6B). Cells treated with ABT888 and CPT-11 showed an

Table 3. Correlation analysis of ATM expression with that of P53, P21, and PUMA

	TCGA cohort ($n = 291$)		P53 wild-type ($n = 152$)		P53 mutant ($n = 134$)	
	r	*P* value	*r*	*P* value	*r*	*P* value
ATM & p53	−0.02	0.72	0.005	0.95	−0.11	0.19
ATM & p21	−0.33	0.00000001*	−0.34	0.00003*	−0.36	0.00002*
ATM & PUMA	−0.19	0.0009*	−0.23	0.005*	−0.17	0.05*

NOTE: *r*, Pearson product–moment correlation coefficient and its associated *P* value.
*Significant correlation in both Spearman and Pearson analyses.

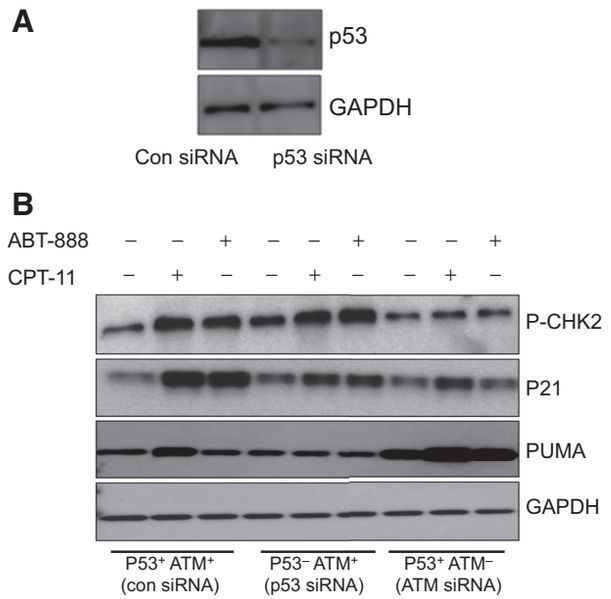

Figure 6.

A, P53 was knocked down in HGC27 cells using targeted siRNAs. (Con siRNA: scrambled controls, p53 siRNA: kd variant). GAPDH served as loading control. **B,** P53 and ATM knocked down HGC27 cells treated with ABT-888 or CPT-11 either as alone or in combination, and its effect in expression of CHK2, P21, and PUMA was detected by immunoblot analysis. Cells treated with scrambled siRNA (Con siRNA) served as experimental control and GAPDH served as loading control.

upregulation of phosphorylated CHK2 kinase (p-CHK2), a cell-cycle regulatory protein. Similarly, a drug-induced upregulation was also observed for P21 expression which appeared more prominent with CPT-11 treatment. On the other hand, kd of ATM leads to a reversal of CHK2 expression to a basal level as comparable with untreated cells. A reduction in P21 expression was also observed in ATM kd cells, hence suggesting a regulatory role of ATM in drug-induced upregulation of check point regulation and cell-cycle arrest. Moreover, ATM was also shown to play a role in drug-induced apoptosis as its loss of expression leads to an upregulation of PUMA. Of interest is the expression of P21 and PUMA in P53 kd cells. Although P21 and PUMA are known downstream targets of P53 (36, 37), loss of P53 expression did not show any significant decrease in the expression of P21 and PUMA. Taken together, the data suggest an ATM-mediated but P53-independent regulation of P21 and PUMA in cells treated with PARP and TOP1 inhibitors.

In-vivo efficacy of CPT-11 and ABT-888 in gastric cancer xenograft model

To characterize the therapeutic potential of ATM targeting in gastric cancer, HGC 27 cells were infected with lentiviruses expressing shRNAs directed against ATM. Lentivirus-infected cells were selected with puromycin, and ATM kd was confirmed by RT-PCR. As shown in Fig. 7A, ATM expression was significantly reduced in shRNA-targeted cells as compared with the cells infected with control shRNA vectors. Stable kd variants of HGC27 cells that showed maximum reduction in ATM expression was selected for further studies. Mice engrafted with HGC27 ATM kd and parental HGC27 control cells showed differential sensitivity to treatment with CPT-11 and ABT-888 (Fig. 7B). No appreciable toxicity was observed in mice as indicated by the absence of significant change in overall body weight. Animals engrafted with HGC27 control cells were more sensitive to CPT-11 monotherapy with a TGI of 70% as compared with 58% TGI in animals treated with ABT-888. On the other hand, combinatorial treatment resulted in a further increase in sensitivity with 79% inhibition of tumor growth. However, mice bearing ATM-deficient tumors (HGC27-ATM kd) showed a greater reduction in tumor growth in response to monotherapy regimens with a TGI of 83% and 70% for CPT-11 and ABT-888, respectively. This suggests enhanced sensitivity of TOP1 and PARP inhibitors in ATM-deficient tumors, where combinatorial treatment with a TGI of 77% did not provide an increase in therapeutic benefit.

Discussion

The challenge in cancer chemotherapy is to achieve maximum efficacy by overcoming endogenous resistance mechanisms in cancer cells. The capacity of cancer cells to recognize DNA damage and initiate DNA repair is a key mechanism for therapeutic resistance or recurrence. In this regard, the sensitivity of cancer cells to DNA-damaging agents could be attributed to intrinsic expression levels of DNA repair proteins. ATM is a key protein which plays a pivotal role in the initiation of DNA repair pathways. Once activated, ATM phosphorylates a series of substrates to mediate cell-cycle control at G_1–S, in S phase, and at the G_2–M transition (38). Inhibition of DNA repair proteins using targeted inhibitors would cause the accumulation of DNA damage in cancer cell that eventually leads to cell death. However, the efficacy of these compounds could be diminished due to the simultaneous activation of alterative pathways. For instance, Aguilar-Quesada and colleagues (39) demonstrated reduced efficacy of PARP inhibitors in cells with optimal activation of ATM kinase.

In the present study, a reduction in ATM expression was found to be associated with increased drug sensitivity to PARP and TOP1 inhibitors, ABT-888 and CPT-11, respectively. This finding is consistent with and further elaborates studies by Kubota and colleagues and Gilardini Montani and colleagues (22) that showed higher efficacy of PARP inhibitors in ATM-deficient breast cancer cells. The data indicate a mechanism of synthetic lethality where ATM deficiency results in a defective DNA repair pathway that selectively sensitizes cancer cells to PARP and TOP1 inhibitor–induced cell death. Synthetic lethal targeting of cancer cells could be therapeutically advantageous to targeting of cancer cells with standard agents, especially when two parallel pathways both contribute to an essential process. In such a scenario, disruption of a gene in one pathway may not be as lethal, as the alternative pathway can sufficiently maintain the essential process, whereas disruption of both pathways is lethal to the cell (40). However, the relative sensitivity of gastric cancer cells to TOP1 inhibition was higher when compared with PARP inhibition. This could be attributed to innate variations in the drug-induced regulation of DNA repair and cell death. The current study explored the efficacy of combinational therapies to potentiate the effects of PARP and TOP1 inhibitors in gastric cancer treatment. Intriguingly, combinational drug treatment resulted in greater sensitization of gastric cancer cells to DNA-damaging effects of ABT-888 and CPT-11. *In vitro*, a synergistic action between ABT-888 and

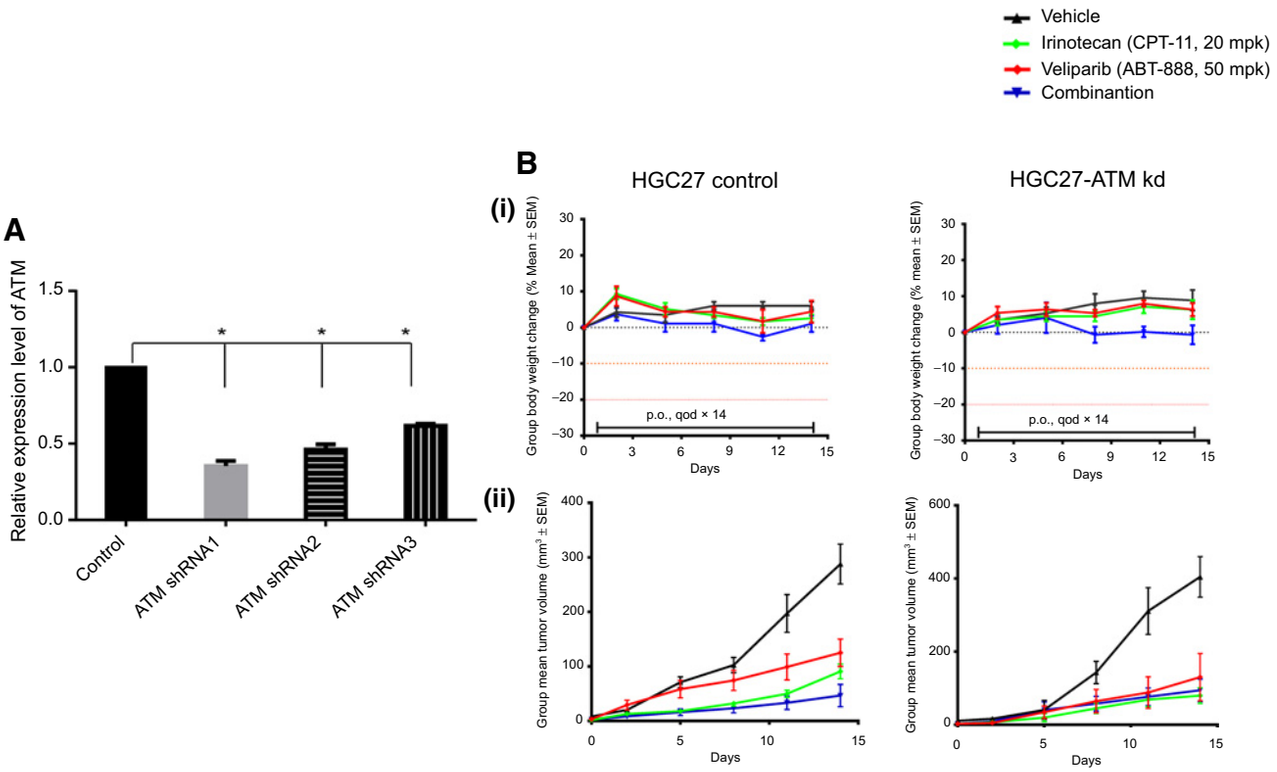

Figure 7.

A, shRNA kd of ATM in HGC 27 cells. Relative expression levels of ATM in cells transfected with different targeted shRNAs. The expression levels were normalized to GAPDH and were compared against cells transfected with control nontargeting shRNAs. The data are representative of at least two independent experiments, and error bars represent SD, *, $P < 0.05$ is considered significant. **B,** CPT-11 and ABT-888 sensitivity in xenograft mice models: NOD-SCID mice were injected subcutaneously with HGC27 control or HGC27-ATM kd cells. Five animals were randomly assigned to each group and treated for 2 weeks with irinotecan and veliparib either as single agent or in combination. **(i)** Evaluation of body weight; **(ii)** Mean tumour volume (mm^3).

CPT-11 was observed in this study that predisposes gastric cancer cells to undergo apoptosis despite having an active ATM-driven DNA repair mechanism. Moreover, high expression level of ATM was found to be associated with lower effective dose (ED), hence suggesting ATM as a predictive marker for sensitivity to combinational chemotherapy using ABT-888 and CPT-11. The sensitivity observed in low ATM-expressing cell lines could be reflective of a more additive effect to individual drugs, while the effects of combination therapy in cell lines that have higher ATM expression reflect stronger synergistic interactions. Previously, Taverna and colleagues (41) showed that inhibition of base excision repair (BER) contributes to sensitivity of mammalian cells to DNA damage insults. In mammalian cells, PARP is a known activator of BER during DNA damage. Hence, inhibition of PARP would contribute to reduced BER capacity (39). Therefore, it is befitting to reason that when the PARP-induced BER activity is inhibited by ABT-888, dsDNA breaks induced by CPT-11 could result in enhanced accumulative DNA damage, thereby causing enhanced sensitivity to cellular apoptosis. However, it remains uncharacterized whether these drugs in combination have any direct repressive effect on ATM activation. Notably, the enhanced efficacy observed in combinational treatment was independent of ATM deficiency and appeared more significant in high ATM-expressing cells. Because previous studies have shown high ATM expression being associated with poor drug response and clinical outcome, our study is suggestive of a potential therapeutic approach that could overcome ATM-induced activation of DNA repair signaling and induce maximum efficacy in anti-cancer therapy.

The mechanism of ATM-induced synthetic lethality is also investigated in this study. ATM-induced DNA damage response is primarily mediated through the tumor-suppressor protein P53. In response to DNA-damaging insults, ATM together with its downstream target CHK2 phosphorylates P53 that leads to its stabilization in the cell nucleus. Once activated and stabilized in the nucleus, P53 acts as a transcription factor and drives the expression of genes involved in cell-cycle arrest, such as p21 and also genes involved in induction of apoptosis. However, in the present study, we have shown significant upregulation of P21 in P53 kd cells treated with CPT-11. Interestingly, ATM depletion leads to a total reversal of p21 upregulation in CPT-11–treated cells. This suggests a role of ATM in P53-independent activation of P21. The inverse correlation between ATM with that of P21 and PUMA in clinical samples is also suggestive of a P53-independent regulatory role of ATM in gastric cancer. Our findings add further credence to the study by Luo and colleagues (3) that showed the mediatory role of ATM in direct phosphorylation of P21 in a P53-independent manner. Phosphorylation of p21 promotes its nucleo cytoplasmic translocation and subsequent ubiquitin-dependent degradation (42). Apart from this, ATM depletion also resulted in enhanced sensitivity of gastric cancer cells TOP1

and PARP inhibitors. This indicates a contributory role of ATM in CPT-11 and ABT-888 sensitivity, through the negative regulation of proapoptotic PUMA protein. Moreover, the upregulation of H2AX in cells treated with TOP1 and PARP inhibitors also suggests enhanced DNA repair activity induced by ATM. It could therefore be inferred that DNA-damaging agents would show a lesser sensitivity in ATM-expressing cells due to the induction of cell-cycle check point activation and DNA damage repair through the upregulation of CHK2 and P21 proteins. On the other hand, depletion of ATM would cause a shift in cellular homeostasis from check point activation to apoptosis and leads to enhanced drug sensitivity through the upregulation of PUMA and downregulation of P21 and CHK2 Proteins.

The conclusion drawn from the *in-vitro* study was further confirmed in *in-vivo* xenograft models of gastric cancer as ATM deficiency rendered the cells more sensitive to PARP and TOP1 inhibition. However, the data are also suggestive of the enhanced efficacy of combinatorial regimens in ATM-driven cancers. In summary, this study highlights the clinical utility of ATM expression as a synthetically lethal and predictive marker for sensitivity of gastric cancer cell to PARP and TOP1 inhibition. Also, we demonstrate combinational therapy using PARP and TOP1 inhibitors as a therapeutic strategy that would enhance drug efficiency as well as sensitivity of gastric cancer cells to chemotherapy in ATM-driven cancers. Our study also identifies a novel functional role of ATM in gastric cancer cells, where it mediates a P53-independent regulation of cell cycle and apoptosis. Future studies should aim to identify specific alteration in DNA repair pathways that coexists in ATM-deficient cancers so as to achieve better and predictable prognosis through tailored therapeutic regimens.

Disclosure of Potential Conflicts of Interest

W.P. Yong is a consultant/advisory board member for Aslan Pharmaceuticals. No potential conflicts of interest were disclosed by the other authors.

Authors' Contributions

Conception and design: V.V. Subhash, W.P. Yong
Development of methodology: V.V. Subhash, V. Krishnan
Acquisition of data (provided animals, acquired and managed patients, provided facilities, etc.): V.V. Subhash, F.L. Yan, P.C. Peethala, N. Liem
Analysis and interpretation of data (e.g., statistical analysis, biostatistics, computational analysis): V.V. Subhash, S.H. Tan, F.L. Yan, V. Krishnan, W.P. Yong
Writing, review, and/or revision of the manuscript: V.V. Subhash, M.S. Yeo, W.P. Yong
Study supervision: V.V. Subhash, W.P. Yong

Acknowledgments

The authors would like to thank the anonymous reviewers for their valuable comments and suggestions to improve the quality of the article.

Grant Support

This study was funded by the translational research grant awarded to Dr. W.P. Yong by the National Medical Research Council (NMRC), Singapore (Grant number: NMRC/TCR/009-NUH/2013).

The costs of publication of this article were defrayed in part by the payment of page charges. This article must therefore be hereby marked *advertisement* in accordance with 18 U.S.C. Section 1734 solely to indicate this fact.

Received December 24, 2015; revised August 26, 2016; accepted August 26, 2016; published OnlineFirst September 16, 2016.

References

1. Gately DP, Hittle JC, Chan GK, Yen TJ. Characterization of ATM expression, localization, and associated DNA-dependent protein kinase activity. Mol Biol Cell 1998;9:2361–74.
2. Lavin MF, Kozlov S. ATM activation and DNA damage response. Cell Cycle 2007;6:931–42.
3. Luo X, Suzuki M, Ghandhi SA, Amundson SA, Boothman DA. ATM regulates insulin-like growth factor 1-secretory clusterin (IGF-1-sCLU) expression that protects cells against senescence. PLoS One 2014;9:e99983.
4. Cremona CA, Behrens A. ATM signalling and cancer. Oncogene 2014;33:3351–60.
5. Millour J, de Olano N, Horimoto Y, Monteiro LJ, Langer JK, Aligue R, et al. ATM and p53 regulate FOXM1 expression via E2F in breast cancer epirubicin treatment and resistance. Mol Cancer Ther 2011;10:1046–58.
6. Knappskog S, Chrisanthar R, Lokkevik E, Anker G, Ostenstad B, Lundgren S, et al. Low expression levels of ATM may substitute for CHEK2 /TP53 mutations predicting resistance towards anthracycline and mitomycin chemotherapy in breast cancer. Breast Cancer Res 2012;14:R47.
7. Hosoya N, Miyagawa K. Targeting DNA damage response in cancer therapy. Cancer Sci 2014;105:370–88.
8. Goode EL, Ulrich CM, Potter JD. Polymorphisms in DNA repair genes and associations with cancer risk. Cancer Epidemiol Biomarkers Prev 2002;11:1513–30.
9. Lomax ME, Folkes LK, O'Neill P. Biological consequences of radiation-induced DNA damage: Relevance to radiotherapy. Clin Oncol (R Coll Radiol) 2013;25:578–85.
10. Bouwman P, Jonkers J. The effects of deregulated DNA damage signalling on cancer chemotherapy response and resistance. Nat Rev Cancer 2012;12:587–98.
11. Ding L, Getz G, Wheeler DA, Mardis ER, McLellan MD, Cibulskis K, et al. Somatic mutations affect key pathways in lung adenocarcinoma. Nature 2008;455:1069–75.
12. Seshagiri S, Stawiski EW, Durinck S, Modrusan Z, Storm EE, Conboy CB, et al. Recurrent R-spondin fusions in colon cancer. Nature 2012;488:660–4.
13. Meyer A, John E, Dork T, Sohn C, Karstens JH, Bremer M. Breast cancer in female carriers of ATM gene alterations: Outcome of adjuvant radiotherapy. Radiother Oncol 2004;72:319–23.
14. Kim JW, Im SA, Kim MA, Cho HJ, Lee DW, Lee KH, et al. Ataxia-telangiectasia-mutated protein expression with microsatellite instability in gastric cancer as prognostic marker. Int J Cancer 2014;134:72–80.
15. Roossink F, Wieringa HW, Noordhuis MG, Ten Hoor KA, Kok M, Slagter-Menkema L, et al. The role of ATM and 53BP1 as predictive markers in cervical cancer. Int J Cancer 2012;131:2056–66.
16. Palmieri D, Valentino T, D'Angelo D, De Martino I, Postiglione I, Pacelli R, et al. HMGA proteins promote ATM expression and enhance cancer cell resistance to genotoxic agents. Oncogene 2011;30:3024–35.
17. Wagner LM. Profile of veliparib and its potential in the treatment of solid tumors. Onco Targets Ther 2015;8:1931–9.
18. Weil MK, Chen AP. PARP inhibitor treatment in ovarian and breast cancer. Curr Probl Cancer 2011;35:7–50.
19. Horton JK, Watson M, Stefanick DF, Shaughnessy DT, Taylor JA, Wilson SH. XRCC1 and DNA polymerase beta in cellular protection against cytotoxic DNA single-strand breaks. Cell Res 2008;18:48–63.
20. Nowsheen S, Yang ES. The intersection between DNA damage response and cell death pathways. Exp Oncol 2012;34:243–54.
21. Shaheen M, Allen C, Nickoloff JA, Hromas R. Synthetic lethality: exploiting the addiction of cancer to DNA repair. Blood 2011;117:6074–82.
22. Gilardini Montani MS, Prodosmo A, Stagni V, Merli D, Monteonofrio L, Gatti V, et al. ATM-depletion in breast cancer cells confers sensitivity to PARP inhibition. J Exp Clin Cancer Res 2013;32:95.
23. Kubota E, Williamson CT, Ye R, Elegbede A, Peterson L, Lees-Miller SP, et al. Low ATM protein expression and depletion of p53 correlates with olaparib sensitivity in gastric cancer cell lines. Cell Cycle 2014;13:2129–37.

24. Davidson D, Wang Y, Aloyz R, Panasci L. The PARP inhibitor ABT-888 synergizes irinotecan treatment of colon cancer cell lines. Invest New Drugs 2013;31:461–8.
25. Gibson RJ, Stringer AM, Bowen JM, Logan RM, Yeoh AS, Burns J, et al. Velafermin improves gastrointestinal mucositis following irinotecan treatment in tumor-bearing DA rats. Cancer Biol Ther 2007;6:541–7.
26. Gilbert DC, Chalmers AJ, El-Khamisy SF. Topoisomerase I inhibition in colorectal cancer: Biomarkers and therapeutic targets. Br J Cancer 2012; 106:18–24.
27. Ray Chaudhuri A, Hashimoto Y, Herrador R, Neelsen KJ, Fachinetti D, Bermejo R, et al. Topoisomerase I poisoning results in PARP-mediated replication fork reversal. Nat Struct Mol Biol 2012;19:417–23.
28. Tentori L, Leonetti C, Scarsella M, Muzi A, Mazzon E, Vergati M, et al. Inhibition of poly(ADP-ribose) polymerase prevents irinotecan-induced intestinal damage and enhances irinotecan/temozolomide efficacy against colon carcinoma. FASEB J 2006;20:1709–11.
29. Kummar S, Chen A, Ji J, Zhang Y, Reid JM, Ames M, et al. Phase I study of PARP inhibitor ABT-888 in combination with topotecan in adults with refractory solid tumors and lymphomas. Cancer Res 2011; 71:5626–34.
30. Smith LM, Willmore E, Austin CA, Curtin NJ. The novel poly(ADP-Ribose) polymerase inhibitor, AG14361, sensitizes cells to topoisomerase I poisons by increasing the persistence of DNA strand breaks. Clin Cancer Res 2005;11:8449–57.
31. Curtin N. PARP inhibitors for anticancer therapy. Biochem Soc Trans 2014;42:82–8.
32. Xu Y, Her C. Inhibition of topoisomerase (DNA) I (TOP1): DNA damage repair and anticancer therapy. Biomolecules 2015;5:1652–70.
33. Yang X, Boehm JS, Salehi-Ashtiani K, Hao T, Shen Y, Lubonja R, et al. A public genome-scale lentiviral expression library of human ORFs. Nat Methods 2011;8:659–61.
34. Rahko E, Blanco G, Soini Y, Bloigu R, Jukkola A. A mutant TP53 gene status is associated with a poor prognosis and anthracycline-resistance in breast cancer patients. Eur J Cancer 2003;39:447–53.
35. Bertheau P, Turpin E, Rickman DS, Espie M, de Reynies A, Feugeas JP, et al. Exquisite sensitivity of TP53 mutant and basal breast cancers to a dose-dense epirubicin-cyclophosphamide regimen. PLoS Med 2007;4(3):e90.
36. Nakano K, Vousden KH. PUMA, a novel proapoptotic gene, is induced by p53. Mol Cell 2001;7:683–94.
37. Rahman-Roblick R, Roblick UJ, Hellman U, Conrotto P, Liu T, Becker S, et al. p53 targets identified by protein expression profiling. Proc Natl Acad Sci U S A 2007;104:5401–6.
38. Iliakis G, Wang Y, Guan J, Wang H. DNA damage checkpoint control in cells exposed to ionizing radiation. Oncogene 2003;22:5834–47.
39. Aguilar-Quesada R, Munoz-Gamez JA, Martin-Oliva D, Peralta A, Valenzuela MT, Matinez-Romero R, et al. Interaction between ATM and PARP-1 in response to DNA damage and sensitization of ATM deficient cells through PARP inhibition. BMC Mol Biol 2007;8:29.
40. Chan DA, Giaccia AJ. Harnessing synthetic lethal interactions in anticancer drug discovery. Nat Rev Drug Discov 2011;10:351–64.
41. Taverna P, Hwang HS, Schupp JE, Radivoyevitch T, Session NN, Reddy G, et al. Inhibition of base excision repair potentiates iododeoxyuridine-induced cytotoxicity and radiosensitization. Cancer Res 2003;63: 838–46.
42. Child ES, Mann DJ. The intricacies of p21 phosphorylation: Protein/protein interactions, subcellular localization and stability. Cell Cycle 2006;5:1313–9.